

Advanced Technique for Three-Dimensional Visualization of Compound Distributions in a Rice Kernel

Yukiharu Ogawa,^{*,†} Junichi Sugiyama,[†] Heinrich Kuensting,[†] Toshio Ohtani,[†] Shoji Hagiwara,[†] XinQi Liu,[‡] Mitsunori Kokubo,[§] Akio Yamamoto,[#] Ken-ichi Kudoh,[#] and Toshiro Higuchi[#]

National Food Research Institute, 2-1-2 Kannondai, Tsukuba, 305-8642 Japan; Advanced Science Research Center, Japan Atomic Energy Research Institute, 2-4 Shirane, Tokai, 319-1195 Japan; Research and Development Center, Toshiba Machine Company, Ltd., 2068-3 Ooka, Numazu, 410-8510 Japan; and School of Engineering, The University of Tokyo, 7-3-1 Hongo, Bunkyo, 113-8656 Japan

A three-dimensional (3D) visualization technique for the compound distribution in a rice kernel was developed. This technique is a combination of sectioning, staining, and digital image postprocessing. By using a special microtome system with adhesive tapes, a set of sequential sections of a rice kernel, which can be preserved with their own set of relative position data, was obtained. A single set of sequential sections was stained by various chemical techniques for the visualization of protein, starch, or lipid content. Each stained section was digitally captured using a CCD imaging device. As the stained areas represent areas containing dye–target complex, the distribution of each compound in the section was visualized in two dimensions. The digitally captured images of a single set of sequential sections were reconstructed to produce a 3D plotting image. As a result, the distributions of various compounds in a rice kernel could be visualized in a new 3D model.

Keywords: 3D; distribution; protein; starch; lipid; staining; rice kernel

INTRODUCTION

To evaluate the quality or safety of agricultural products and foodstuffs and to elucidate migration processes of compounds, the internal composition is important. For the investigation of such compositions, microscopy with sectioning method has been applied to a small part of material in former days (1–5). The large-scale imaging method for the measurement of the cross section of agricultural products has also been studied (6–8). These research results are analyzed and represented by two-dimensional (2D) imaging. Because the form of agricultural products or foodstuffs is three-dimensional (3D), a 3D analysis method for the compositions, especially for the distribution of chemical compounds, is required for a thorough evaluation.

The 3D imaging method using optical sectioning techniques (9–12) or confocal laser scanning microscopes with a fluorescent staining method in a thin section of material for the measurement of the physical structure and compound distribution of small areas, which are suitable for microscopic observation, has been studied (13–17). These methods allow the 3D visualization of the distribution of chemical compounds in small parts of the material. However, the measurement of large-scale 3D distributions, such as the distribution of chemical compounds throughout the whole body of harvest goods, has not been achieved by its principal limits. Nuclear magnetic resonance (NMR) can be used

to measure such large-scale distributions of particular compounds using characteristic proton shifts in a material (18–20). By applying magnetic resonance imaging (MRI), their distribution can be measured rendering 2D images or the 3D plotting images constructed from such 2D images (21). However, MRI could not achieve the determination of various compounds by its principal properties.

For the measurement of the internal composition of a material, the traditional sectioning technique using a microtome has been applied as mentioned above. Although this sectioning technique is destructive, the distribution of various chemical compounds in a section can be visualized and analyzed in 2D by special staining or other imaging methods. To observe the internal composition in 3D, in past days such sectioning methods with computer aid for the 3D reconstruction of serial section images using their interactive formation were applied to measure the 3D physical structure of the central nervous system of a simple animal (22) and plant cells (23). Because the interactive formation method for 3D reconstructions of sequential sections is based on the outline of the object to be constructed, it is suitable not for the compound distributions but for physical structures.

By using such traditional sectioning techniques and digital imaging technology, an advanced technique for the 3D visualization of compound distributions in an organic body is developed. This process is a combination of sectioning methods to obtain sequential sections by a special microtome system with a position fixing device, staining by chemical methods, 2D digital imaging, and 3D reconstruction by stacking of 2D digital images. A grain of brown rice (*Oryza sativa* L.), which has a scale suitable for the current sectioning device and imaging facilities, was used to test for such advanced techniques.

* Author to whom correspondence should be addressed (e-mail ogw@nfri.affrc.go.jp; telephone +81-298-38-8047; fax +81-298-39-1552).

[†] National Food Research Institute.

[‡] Japan Atomic Energy Research Institute.

[§] Toshiba Machine Co. Ltd.

[#] The University of Tokyo.

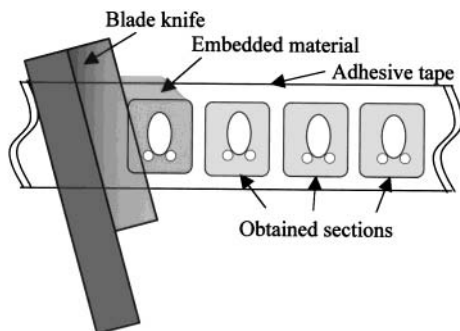


Figure 1. Schematic diagram of the sectioning method with an adhesive tape.

In this study, the protein, starch, or lipid distributions in a rice kernel were visualized three-dimensionally.

MATERIALS AND METHODS

Materials. Brown rice grains (cv. Nipponbare) harvested in 1998 in the Tsukuba region, Ibaraki Prefecture, Japan, were used for this experiment. Positioning rods were used to adjust the position of all 2D images to reconstruct a 3D data set. As these positioning rods so-called "somen" are used, which are a kind of Japanese dried noodle, similar to Italian spaghetti. Their diameter is ~ 1 mm, their color is white, and their form is cylindrical. Special adhesive tapes, which are made of polyester (PET) and coated with a solvent-type acrylic resin as the adhesive material, are used to obtain sections in sequence.

Embedding. To prepare for sectioning, a rice kernel was directly embedded in paraffin. Two positioning rods were also carefully embedded with their long axis perpendicular to the bottom plane of the embedding mold. The temperature of liquid paraffin was kept at 60°C during the embedding procedure.

Sectioning. The embedded materials, including a rice kernel and the two positioning rods, were sliced by an automatic precision microtome system (Toshiba Machine Co., Ltd.). This system provides a higher precision in comparison to ordinary microtomes (24). The obtained sequential sections from the embedded material are preserved by adhesion onto tapes. Each adhered section contained slices of a rice kernel, of two positioning rods, and of the paraffin surrounding the rice section. Figure 1 shows a schematic diagram of the sectioning method with an adhesive tape. By this method, each section retains its position relative to the order of all slices. The thickness of all sections in this experiment was $20.0\ \mu\text{m}$.

Staining. To visualize protein, starch, or lipid in each rice section, a chemical staining method was applied to each set of the sequential sections.

For the protein visualization, a single set of sequential sections was fixed with a solution of 4% (w/v) paraformaldehyde (in phosphate buffer, pH 7.4) before staining. The fixing time was 2 min at room temperature. Fixed sections were soaked with Coomassie brilliant blue (CBB) solution (see below) for 2 min and then washed exhaustively with a solution of 20% methanol and 7% acetic acid in distilled water at 25°C . [Note: CBB R-250 (1.25 g) was dissolved in 250 mL of methanol and 50 mL of acetic acid. The resulting solution was diluted to a final volume of 500 mL by distilled water. This solution was used as CBB solution.]

For the starch visualization, a single set of sequential sections was fixed with a solution of 10% formaldehyde directly before staining. The fixing time was 2 min at room temperature. Fixed sections were soaked with 0.01 N iodine solution for 30 s and then washed exhaustively with distilled water at 25°C .

For the lipid visualization, a single set of sequential sections was fixed with a solution of 10% formaldehyde [including 1.0% (w/v) CaCl_2] before staining. The fixing time was 2 min at room temperature. Fixed sections were rinsed with a solution of 50% ethanol in water for 1 min and then soaked with Sudan black

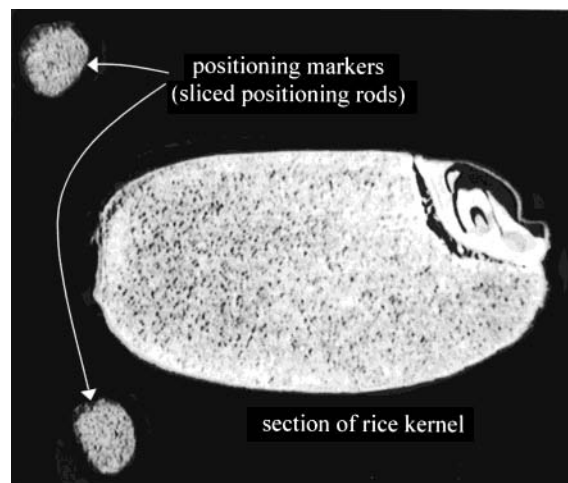


Figure 2. Sample image of a rice section and positioning markers.

B solution (see below) for 7 min at 37°C . The stained sections were washed exhaustively with 50% ethanol twice for 3 min each and then rinsed with distilled water. [Note: Sudan black B (0.5 g) was dissolved in a 500 mL solution of 70% ethanol in water. This solution was used as Sudan black B solution.]

In the cases of protein and starch visualization, the sliced paraffin object was removed by xylene after staining for reduction of optical background noise in the 2D images.

2D Imaging. Each stained section was captured by a CCD imaging device with a ring light system for uniform lighting conditions (CCD-f2, Shimadzu Rika Instrument Co. Ltd.) and digitally imaged by the digital imaging system (DF-20, Fuji-film). The 2D digital images have 24-bit RGB scale. The size of one pixel of the obtained 2D digital images is $13.0 \times 13.0\ \mu\text{m}$.

3D Reconstruction. The obtained 2D digital images were reconstructed to produce a 3D data set by the volume rendering method, which can be plotted on the display for 3D visualization, using special software (Voxel Viewer, Toshiba Machine Co. Ltd.). Therefore, the voxel data, which were produced by pixel data and the thickness of the sections, can represent the position of compounds in a reconstructed rice kernel. The size of one voxel of the produced 3D data set was $20.0 \times 13.0 \times 13.0\ \mu\text{m}$ in this study.

RESULTS AND DISCUSSION

Sectioning Material. All embedded materials were sliced by an ordinary steel knife (Feather Co., S35 type), which set on our microtome system. All obtained sections from an embedded material were adhered onto an adhesive tape (see Figure 1). Figure 2 shows a sample image of an obtained section from an embedded material including a rice section with sliced positioning rods as positioning markers. In this sample image, the paraffin was removed by xylene to improve imaging quality. All objects were adhered onto an adhesive tape. Therefore, the relative position between the rice section and the markers is fixed. Because the positioning rods were embedded with the rice kernel, all sections of a sequential section set were equipped with such positioning markers. Although the captured positions of section images imaged by the CCD imaging device differed from each other, the relative position between each sequential section could be adjusted by referring to two positioning markers.

Staining. Protein, starch, or lipid in each section was visualized by suitable staining methods. Figure 3 shows some sample images of the stained sections after the application of each staining method. The whole images

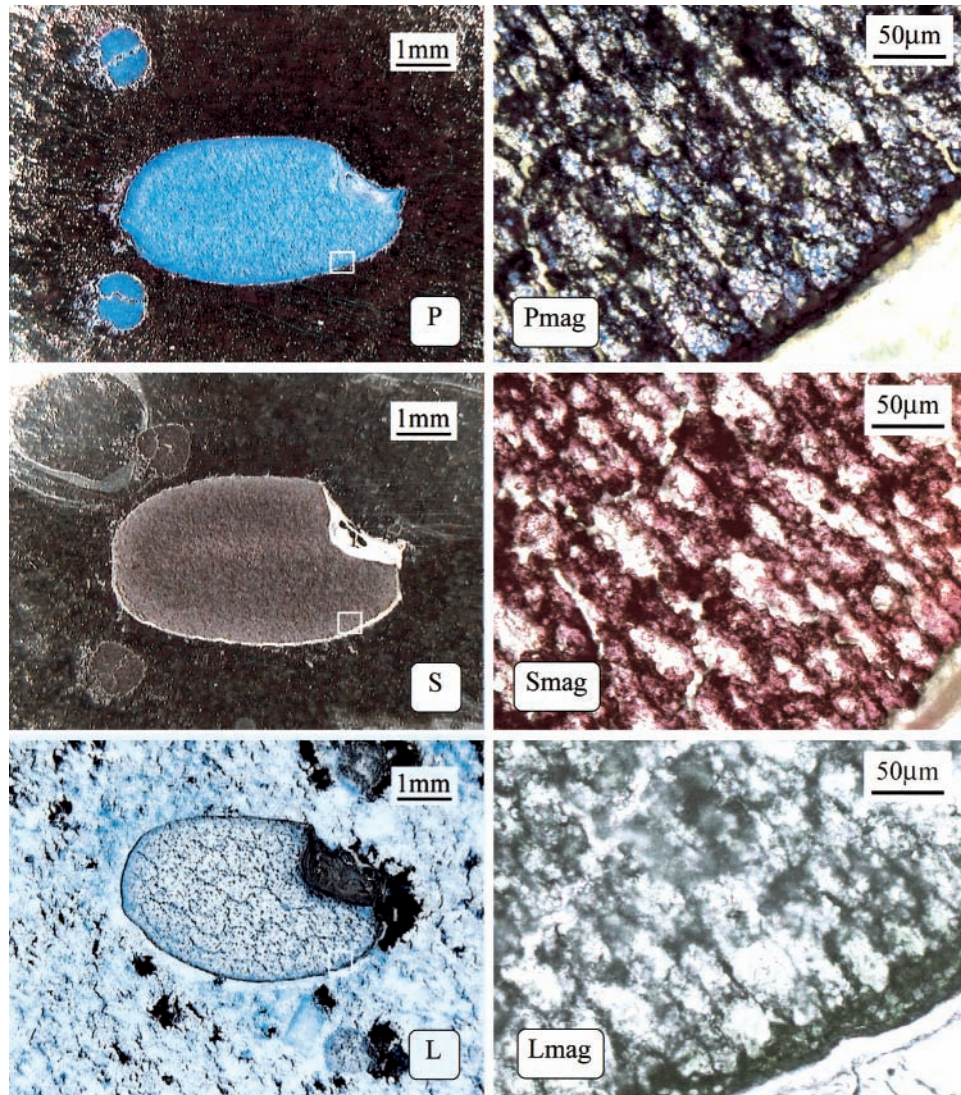


Figure 3. Some sample images of the stained sections of the rice kernel after application of each staining method (left side) and magnifications of each boxed area in the left side (right side). The protein (P, top), starch (S, middle), or lipid (L, bottom) distributions in a section are represented in this figure.

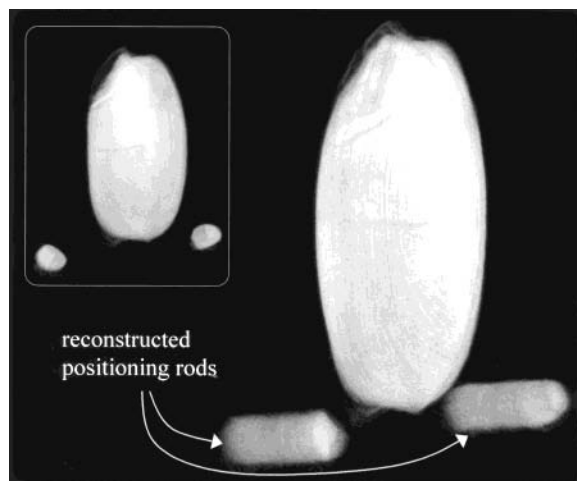


Figure 4. 3D plotting image of a rice kernel and two positioning rods from a diagonal view reconstructed from a single set of sequential sections (a straight view is shown in the box).

of each stained section are shown on the left side. On the right side, magnifications of each boxed area in left-side images are shown.

Protein was stained blue by CBB (upper blocks in Figure 3). In the magnification (Pmag), blue particles, which are called “protein body”, are shown in the cells and the part of seed coat. Thus, the blue area in the whole image (P) represents the protein distribution. In the whole image (P), all parts of the section are represented blue, but it is shown that the surrounding side of the section is darker than the internal side. Considering the magnification and gatherings of the blue particles, the darker area can be correlated to a higher density of stained protein bodies in comparison with the lighter internal area. This result corresponds with past studies (25, 26).

Starch was stained purple or brown by iodine solution (middle blocks in Figure 3). In the magnification (Smag), purple or brown parts are located at the inner section. Compared with the inner area, the seed coat is not stained purple or brown. In the whole image (S), it is shown that the embryo also is not stained, and the surrounding side of the section is lighter than the internal side except for a center part. This distribution differs from that of the protein.

Lipid was stained black or blue by Sudan black B (bottom blocks in Figure 3). In the magnification (Lmag),

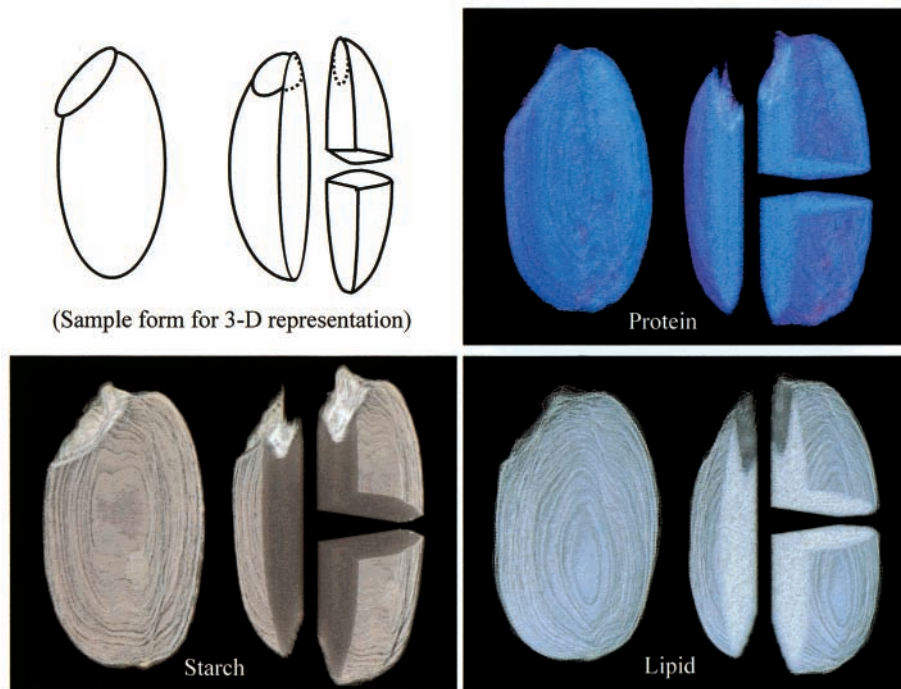


Figure 5. 3D plotting images of each compound distribution, such as protein, starch, or lipid, in a rice kernel.

it is shown that a part of the seed coat is stained black and parts of the inner section are stained light blue. In the whole image (L), the black-stained area of the seed coat and embryo and the blue-stained area in the inner parts of the surrounding side of the section represent the distribution of lipid. This distribution is similar to the protein distribution. The density of the domains of blue in this section decreases from the seed coat to the inner parts of the section. Because lipids are so soluble in xylene, the paraffin surrounding the rice section could not be removed, similar to the case of protein and starch distribution images.

To capture 2D images, all conditions for imaging, such as staining, focusing, lighting, and shuttering, for each single set of sequential sections were standardized.

Reconstruction of the 3D Data Set. To produce a 3D data set, all 2D images of a set of sequential sections were adjusted according to their relative positions based on the adhered positioning markers at the adhesive tape. Adjusted 2D digital images were stacked in the memory of a personal computer by the volume rendering method to represent a 3D plotting image of the produced 3D data set. Figure 4 shows a 3D plotting image from a single set of nonstained sequential sections. (Note: Figure 2 shows one of them.) For a clear 3D representation, an opaque algorithm, which can set up the opacity ratio of the 3D plotting image to let the back side shine through the front side, was applied to the 3D data set. The ratio of opacity set up 1/10 in this image. Positioning rods, shown in this figure, were reconstructed from adjusted positioning markers. Because the positioning markers had relative positions to the sliced rice kernel on the adhesive tape, the rice kernel was also reconstructed in 3D.

The 3D plotting images of the compound distributions in a rice kernel are shown in Figure 5. They were reconstructed by 2D distribution images of a single set of stained sequential sections for each compound. (Note: Sample 2D images of them were shown in Figure 3.) As a result, the compound distribution in a rice

kernel was visualized in 3D. The direction of the embryo of the rice kernel points toward the top of this figure. Each image for the compound distribution represents the whole image (left side in each compound figure) and its virtually divided image (right side; see sample form for 3D representation). The ratio of opacity of these 3D plotting images is also set up 1/10. For the improvement of color differentiation, the image-processing techniques of suitable color emphasis are applied to processed 3D plotting images. The wrinkles in the 3D plotting images, which look like the contour lines of a contour map, are caused by section thickness. This is a peculiarity of this visualization technique. In the 3D plotting image for the protein distribution, it can be shown that the darker area, which represents a concentration area of blue particles shown in the stained 2D image (see Figure 3), is located in the surrounding parts of the whole rice kernel and embryo. By means of 3D model development we can prove that the starch or lipid distributions in a rice kernel behave in the manner that has been only deduced from 2D methods until now. (Note: Because the paraffin surrounding the rice section in 2D images for lipid distribution shown in Figure 3 acts as optical background noise, it is removed manually in the digital images.)

Conclusions. The distributions of the protein, starch, and lipid in a rice kernel in 3D were visualized by using a new 3D visualization technique. The methods of fixing sections in their location with adhesive tapes, 2D imaging with staining, and 3D reconstruction with volume rendering were organized to develop our technique.

The following methods were developed.

(1) By using adhesive tapes and embedded positioning rods, a single set of sequential sections from a rice kernel can be fixed and adjusted in their relative positions.

(2) By application of suitable staining methods for each compound (such as protein, starch, or lipid) and digital capturing by a CCD imaging device, the 2D

digital images of a compound distribution in the whole section, which are represented as differences of the color gradient, were obtained.

(3) By stacking of the 2D digital images of a set of stained sequential sections, which are adjusted in their relative positions, the 3D compound distributions of a rice kernel were visualized.

Not only the compound distribution in a rice kernel but also physiological function, for example, location of the phenotypic expression, can be revealed by using our visualization technique.

LITERATURE CITED

- (1) Rosario, A. R. del; Briones, V. P.; Vidal, A. J.; Juliano, B. O. Composition and endosperm structure of developing and mature rice kernel. *Cereal Chem.* **1968**, *45*, 225–235.
- (2) Saio, K.; Kondo, K.; Sugimoto, T. Changes in typical organelles in developing cotyledons of soybean. *Food Microstruct.* **1985**, *4*, 191–198.
- (3) Yiu, S. H. Cereal structure and its relationship to nutritional quality. *Food Microstruct.* **1989**, *8*, 99–113.
- (4) Yiu, S. H. Food microscopy and the nutritional quality of cereal foods. *Food Struct.* **1993**, *12*, 123–133.
- (5) Irving, D. W.; Jideani, I. A. Microstructure and composition of *Digitaria exilis* stapf (acha): A potential crop. *Cereal Chem.* **1993**, *74*, 224–228.
- (6) Little, R. R.; Hilder, G. B.; Dawson, E. H. Differential effect of dilute alkali on 25 varieties of milled white rice. *Cereal Chem.* **1958**, *35*, 111–126.
- (7) Peterson, D. M.; Wood, D. F. Composition and structure of high-oil oat. *J. Cereal Sci.* **1997**, *26*, 121–128.
- (8) Sugiyama, J. Visualization of sugar content in the flesh of a melon by near-infrared imaging. *J. Agric. Food Chem.* **1999**, *47*, 2715–2718.
- (9) Streibl, N. Three-dimensional imaging by a microscope. *J. Opt. Soc. Am. A* **1985**, *2*, 121–127.
- (10) Nemoto, I. Three-dimensional imaging in microscopy as an extension of the theory of two-dimensional imaging. *J. Opt. Soc. Am. A* **1988**, *5*, 1848–1851.
- (11) Sheppard, C. J. R.; Mao, X. Q. Three-dimensional imaging in a microscope. *J. Opt. Soc. Am. A* **1989**, *6*, 1260–1269.
- (12) Joshi, S.; Miller, M. I. Maximum a posteriori estimation with good's roughness for three-dimensional optical-sectioning microscopy. *J. Opt. Soc. Am. A* **1993**, *10*, 1848–1851.
- (13) Heertje, I.; Vlist, P. van der; Blonk, J. C. G.; Hendrickx, H. A. C. M.; Brakenhoff, G. J. Confocal scanning laser microscopy in food research: some observations. *Food Microstruct.* **1987**, *6*, 115–120.
- (14) Hassan, A. N.; Frank, J. F.; Farmer, M. A.; Schmidt, K. A.; Shalabi, S. I. Formation of yogurt microstructure and three-dimensional visualization as determined by confocal scanning laser microscopy. *J. Dairy Sci.* **1995**, *78*, 2629–2636.
- (15) McKenna, A. B. Examination of whole milk powder by confocal laser scanning microscopy. *J. Dairy Res.* **1997**, *64*, 423–432.
- (16) Uchiumi, A.; Takatsu, A.; Teraki, Y. Sensitive detection of trace aluminum in biological tissues by confocal laser scanning microscopy after staining with lumogallion. *Analyst* **1998**, *123*, 759–762.
- (17) Hutzler, P.; Fischbach, R.; Heller, W.; Jungblut, T. P.; Reuber, S.; Schmitz, R.; Veit, M.; Weissenbock, G.; Schnitzler, J.-P. Tissue localization of phenolic compounds in plants by confocal laser scanning microscopy. *J. Exp. Bot.* **1998**, *49*, 953–965.
- (18) Simorre, J.-P.; Caille, A.; Marion, D.; Marion, D.; Ptak, M. Two- and three-dimensional ^1H NMR studies of a wheat phospholipid transfer protein: Sequential resonance assignments and secondary structure. *Biochemistry* **1991**, *30*, 11600–11608.
- (19) Gil, A. M.; Masui, K.; Naito, A.; Tatham, A. S.; Belton P. S.; Saito, H. A ^{13}C -NMR study on the conformational and dynamical properties of cereal seed storage protein, C-hordein, and its model peptides. *Biopolymers* **1997**, *41*, 289–300.
- (20) Crestini, C.; Argyropoulos, D. S. Structural analysis of wheat straw lignin by quantitative ^{31}P and 2D NMR spectroscopy. The occurrence of ester bonds and α -O-4 substructures. *J. Agric. Food Chem.* **1997**, *45*, 1212–1219.
- (21) Schrader, G. W.; Litchfield, J. B.; Schmidt, S. J. Magnetic resonance imaging applications in the food industry. *Food Technol.* **1992**, *12*, 77–83.
- (22) Levinthal, C.; Ware, R. Three-dimensional reconstruction from serial sections. *Nature* **1972**, *236*, 207–210.
- (23) Tuohy, M.; McConchie, C.; Knox, R. B.; Szarski, L.; Arkin, A. Computer-assisted three-dimensional reconstruction technology in plant cell image analysis: applications of interactive computer graphics. *J. Microsc.* **1987**, *147*, 83–88.
- (24) Kokubo, M.; Higuchi, T.; Kudoh, K.; Fukuda, Y.; Nanto, H. The automatic thin sectioning and staining for light microscopy. The tests by two trial products. *Acta Histochem. Cytochem.* **1999**, *32*, 223–228.
- (25) Houston, D. F.; Iwasaki, T.; Mohammad, A.; Chen, L. Radial distribution of protein by solubility classes in the milled rice kernel. *J. Agric. Food Chem.* **1968**, *16*, 720–724.
- (26) Houston, D. F. The rice caryopsis and its composition. In *Rice: Chemistry and Technology*; American Association of Cereal Chemists: St. Paul, MN, 1972; pp 16–263.

Received for review August 8, 2000. Revised manuscript received November 21, 2000. Accepted November 21, 2000.

JF000997P